

Metal–organic framework with two different types of rigid tricarboxylates: net topology and gas sorption behaviour†

Cite this: *CrystEngComm*, 2013, 15, 9491

Dongwook Kim and Myoung Soo Lah*

Received 27th May 2013,
Accepted 28th June 2013

DOI: 10.1039/c3ce40929e

www.rsc.org/crystengcomm

A 3-dimensional (3-D) anionic metal–organic framework (MOF), $(\text{NH}_2(\text{CH}_3)_2)_3[\text{Zn}_6(\text{BTC})_4(\text{BTB})]$, of an unprecedented 3,3,3,5-c net topology was prepared *via* the solvothermal reaction of the Zn(II) ion with two different types of rigid tricarboxylates, 1,3,5-benzenetricarboxylate (BTC^{3-}) and 1,3,5-benzenetribenzoate (BTB^{3-}), as 3-connected nodes, where a structurally rare $\text{Zn}_2(\text{COO})_5$ cluster serves as a 5-connected secondary building unit. The MOF has a complicated 3-D channel micropore based on three different types of cage-like pores interconnected through the narrow necklike portals of a multiway channel. The MOF that had large solvent-filled pores showed gas sorption behaviour that well matched the pore dimensions and characteristics of the MOF.

Introduction

The diversity of metal–organic frameworks (MOFs) is due to the infinite number of combinations of the building components—the metal ions and organic ligands. However, prediction of the framework structure from the building components is a challenging task.¹ Even a small modification in the building components will result in a MOF with a completely different network structure.

The combination of rigid ligands with a metal ion having a preference for a specific coordination number and geometry could lead to predictable network structures because of the restrained local symmetry of the rigid building components. It is well known that the Cu(II) ion with a carboxylate has a strong preference for a square paddle-wheel cluster $\text{Cu}_2(\text{COO})_4\text{L}_2$ as a 4-, 5-, or 6-connected secondary building unit (SBU) depending on the type of L ligand.² Reaction of the Cu(II) ion and 1,3,5-benzenetricarboxylic acid (H_3BTC) of D_{3h} symmetry, a rigid tricarboxylate ligand with three carboxylate residues in the ligand plane, leads to the MOF of a binodal 3,4-connected **tbo** net topology, Cu-HKUST-1.³ A similar reaction of the Cu(II) ion and 1,3,5-benzenetribenzoic acid (H_3BTB) of D_3 symmetry, another type of rigid

tricarboxylate ligand with three carboxylate residues tilted away from the ligand plane, leads to the MOF of a binodal 3,4-connected **pto** net topology, MOF-14.⁴ The net topologies of Cu-MOFs having other rigid tricarboxylate ligands also depends on the conformations of three carboxylate residues of the ligands. In other words, the net topologies of the MOFs depend on the symmetry of the carboxylate ligands.^{5–7}

The Zn(II) ion has a strong preference for a $\text{Zn}_4\text{O}(\text{COO})_6$ cluster as an SBU in network structures.⁸ However, reactions of the Zn(II) ion with various carboxylic ligands can also generate other diverse carboxylate clusters, $\text{Zn}_3(\text{COO})_6$,⁹ $\text{Zn}_2(\text{COO})_4$,¹⁰ $\text{Zn}_2(\text{COO})_3$,¹¹ and $\text{Zn}_2(\text{COO})_5$,¹² as SBUs, depending on the types of carboxylate ligands and the reaction conditions. Reaction of the Zn(II) ion and 1,4-benzenedicarboxylic acid (H_2BDC), a rigid biscalboxylate ligand, leads to MOF-5 of a 6-connected regular **pcu** net topology, where the $\text{Zn}_4\text{O}(\text{COO})_6$ SBU serves as an octahedral 6-connected node.^{8a} Reaction of the Zn(II) ion and another rigid tricarboxylate ligand, H_3BTB , leads to MOF-177 of a 3,6-connected **qom** net topology with the same 6-connected $\text{Zn}_6\text{O}(\text{COO})_6$ node.^{8c} On the other hand, reaction of the Zn(II) ion with another rigid tricarboxylate ligand, H_3BTC , leads to the MOF of a 3-connected regular **srs** net topology, MOF-4, where not only the ligand, but also $\text{Zn}_2(\text{COO})_3$ SBU, serves as a trigonal 3-connected node.^{11a} Under similar, but slightly modified, reaction conditions, a MOF of a 3,4-connected **tbo** net topology, Zn-HKUST-1, with $\text{Zn}_2(\text{COO})_4$ SBU as a square-planar 4-connected node and the ligand as a trigonal 3-connected node, is generated.^{10h,i}

There are many reports on Zn-MOFs containing both carboxylates and N-donor ligands as two different types of mixed ligands.^{2l,9c,10c,d,g,13} However, there are not many reports on Zn-MOFs with two different kinds of carboxylates as mixed

Interdisciplinary School of Green Energy, Ulsan National Institute of Science & Technology, Ulsan, 689-798, Korea. E-mail: mslah@unist.ac.kr; Fax: +82 52 217 2019; Tel: +82 52 217 2931

† Electronic supplementary information (ESI) available: Table of crystal data and structure refinement, IR spectrum, ¹H NMR spectrum, optical photograph of single crystals, ball-and-stick and network drawing, PXRD data, TGA data, BET- and Langmuir-specific surface area plot data. CCDC 940205. For ESI and crystallographic data in CIF or other electronic format see DOI: 10.1039/c3ce40929e

ligands.^{14–16} Reaction of the Zn(II) ion with mixed biscarboxylates resulted in a MOF of a **pcu** net topology with $Zn_4O(COO)_6$ SBU as a 6-connected node, as in the isorecticular MOFs of MOF-5.^{14a} Reactions of the Zn(II) ion with mixed bis- and triscarboxylates resulted in various 3,6-connected networks of diverse net topologies with $Zn_4O(COO)_6$ SBU as a 6-connected node and the triscarboxylates as 3-connected nodes.^{15a–e} For example, the reaction of the Zn(II) ion with the rigid H_2BDC and H_3BTB ligands of an optimum mole ratio resulted in 3,6-connected UCMC-1 ($[Zn_4O(BDC)(BTB)_{4/3}]$) of a **muo** net topology with $Zn_4O(COO)_6$ SBU as a 6-connected node.^{15a} The reaction of the Zn(II) ion with mixed tris- and tetrakis-carboxylates afforded a MOF of an unprecedented 3,4,6-c net topology with $Zn_4O(COO)_6$ SBU as a 6-connected node, and the tris- and the tetrakis-carboxylates as 3-connected and 4-connected nodes, respectively.¹⁶ However, there are no reports on any Zn-MOFs with two different kinds of rigid triscarboxylates.

Here, we report the preparation of the first Zn-MOF containing the two rigid triscarboxylates, 1,3,5-benzenetricarboxylate (BTC^{3-}) and 1,3,5-benzenetribenzoate (BTB^{3-}), simultaneously, in the framework, and investigate the characteristics of the Zn-MOF, including the type of Zn-carboxylate cluster as an SBU, the network topology, pore structure, and gas sorption behaviour.

Experimental section

General procedures

All reagents were purchased from commercial sources and were used without further purification. Elemental analysis (EA) for C, H, and N was performed using a Thermo Scientific Flash 2000 elemental analyzer. FT-IR spectra were recorded in the range 4000–450 cm^{-1} with a Varian 670 FT-IR spectrophotometer. Powder X-ray diffraction (PXRD) data were recorded using a Bruker D2 Phaser automated diffractometer at room temperature with a step size of 0.02° in 2θ angle. Simulated PXRD patterns were calculated with the Materials Studio program using single-crystal diffraction data.¹⁷ Thermogravimetric analysis (TGA) was performed using a SDT Q600 instrument (TA Instruments, USA) under N_2 with a heating rate of 5 °C min^{-1} between ambient temperature and 600 °C.

Synthesis of the MOF

$(NH_2(CH_3)_2)_3[Zn_6(BTC)_4(BTB)] \cdot xDMA \cdot yH_2O$ (**1**), where x and y are the numbers of molecules of the DMA solvent and water per formula unit, respectively. $Zn(NO_3)_2 \cdot 6H_2O$ (30.7 mg, 0.101 mmol), H_3BTC (21.7 mg, 0.101 mmol) and H_3BTB (22.1 mg, 0.051 mmol) were dissolved in 4 mL anhydrous N,N' -dimethylacetamide (DMA) in a capillary tube. The tube was flame-sealed, heated to 120 °C for 2 weeks, and then slowly cooled to ambient temperature. The block-shaped colorless crystals obtained were soaked in 10 mL fresh DMA for 2 days. The solvent was refreshed more than four times during the soaking period to remove residual reactants from the pores. The activated sample, **1a**, was prepared by soaking the crystals

in 10 mL acetone for 4 days (the soaking solvent was refreshed more than 10 times during the soaking period), and then vacuum-drying at room temperature for 14 h. Yield: 26.3 mg, 27.1%. EA and IR (Fig. S1, ESI†) data were obtained for an activated sample exposed in air for a couple of minutes prior to analysis. EA for $(NH_2(CH_3)_2)_3[Zn_6(BTC)_4(BTB)] \cdot 0.16DMA \cdot 3H_2O$ ($C_{69.64}H_{60.44}N_{3.16}O_{34.16}Zn_6$, fw = 1880.45 $g\ mol^{-1}$). Calculated: C, 44.91; H, 3.16; N, 2.38%. Found: C, 44.61; H, 3.24; N, 2.50%. IR (KBr, cm^{-1}): 3438 (m, b), 3069 (w), 3023 (w), 2961 (w, sh), 2938 (w), 2873 (w), 2811 (w), 2499 (w), 1701 (m, sh), 1631 (vs), 1589 (s, sh), 1509 (m), 1435 (s, sh), 1415 (s, sh), 1401 (s, sh), 1361 (vs), 1263 (m), 1188 (s), 1139 (s), 1102 (s), 1060 (vs), 1017 (m), 964 (vs), 940 (vs), 894 (vs), 859 (s), 810 (s), 785 (s), 767 (m), 725 (m), 670 (vs), 655 (vs), 644 (vs), 632 (vs), 620 (vs), 591 (s), 574 (vs), 563 (vs), 552 (vs), 540 (vs), 527 (vs), 514 (vs), 506 (vs), 473 (s), 453 (s).

Crystallographic data collection and refinement of the structure

A single crystal of **1** was coated with paratone oil and the diffraction data were measured at 100 K with synchrotron radiation ($\lambda = 0.67000$ Å) using an ADSC Quantum-210 detector with a silicon (111) double-crystal monochromator at the Pohang Accelerator Laboratory (2D SMC beamline), Korea. The ADSC Q210 ADX program¹⁸ was used for data collection (detector distance 90 mm, omega scan; $\Delta\omega = 1^\circ$, exposure time 10 s per frame) and HKL3000sm (Ver. 703r)¹⁹ was used for cell refinement, reduction, and absorption correction. The crystal structure was solved by the direct method with the SHELXTL-XS program and refined by full-matrix least-squares calculations with the SHELXTL-XL program package (Ver. 2008).²⁰

1. $(NH_2(CH_3)_2)_3[Zn_2(BTC)_{4/3}(BTB)_{1/3}] (C_{23}H_{17}N_1O_{10}Zn_2)$, fw = 598.12 $g\ mol^{-1}$, cubic, space group $Fd\bar{3}c$, $a = b = c = 62.779(7)$ Å, $V = 247\,422(49)$ Å³, $Z = 192$, μ (synchrotron radiation, $\lambda = 0.67000$ Å) = 0.785 mm^{-1} , 356 572 reflections were collected, 9637 were unique ($R_{int} = 0.0538$). A BTC^{3-} on a general position, another BTC^{3-} on a crystallographic threefold axis, a BTB^{3-} on the other crystallographic threefold axis, and two zinc atoms on general positions are observed as an asymmetric unit. All nonhydrogen atoms are refined anisotropically; the hydrogen atoms attached to the ligands were assigned isotropic displacement coefficients $U(H) = 1.2U(C)$ and their coordinates were allowed to ride on their respective atoms. The refinement converged to $R_1 = 0.1562$ and $wR_2 = 0.4202$ for 6185 reflections with $I > 2\sigma(I)$. Structure refinement after modification of the structure factors for the electron densities corresponding to the solvent molecules and a completely disordered dimethylammonium counteranion in the solvent pore (170 143 Å³, 68.8% of the unit cell volume; 124 electrons correspond to the electrons of one third dimethylammonium ion and ~2.4 DMA molecules (or certain combination of DMA and water molecules) per asymmetric unit) with the SQUEEZE routine of PLATON²¹ led to better refinement and data convergence. Refinement of the structure converged to a final $R_1 = 0.0850$ and $wR_2 = 0.2807$ for 6813 reflections with $I > 2\sigma(I)$,

$R_1 = 0.1064$, and $wR_2 = 0.3095$ for all 9637 reflections. The largest differences in peak and hole were 0.496 and $-0.345 \text{ e } \text{\AA}^{-3}$, respectively.

A summary of the crystal data and some crystallography data is given in Table S1, ESI†. CCDC 940205 contains the supplementary crystallographic data for 1.

Gas sorption measurements

The gas sorption isotherms were measured with an ASAP 2020 (Micromeritics Instrument Corporation) in a standard volumetric technique up to 1 atm. A part of the N_2 adsorption isotherm in the P/P_0 range 0.014358–0.09479 was fitted to the BET equation to estimate the BET-specific surface area. The Langmuir-specific surface area calculation was performed using all adsorption data.

Results and discussion

Preparation of the MOF

The solvothermal reaction of $\text{Zn}(\text{NO}_3)_2 \cdot 6\text{H}_2\text{O}$ with two different kinds of rigid triscarboxylic acids, H_3BTC and H_3BTB , in 2:2:1 mole ratio in anhydrous DMA at 120 °C resulted in a 3-dimensional (3-D) MOF, $(\text{NH}_2(\text{CH}_3)_2)_3[\text{Zn}_6(\text{BTC})_4(\text{BTB})] \cdot x\text{DMA} \cdot y\text{H}_2\text{O}$ (1).† The presence of the countercationic dimethylammonium ion, generated *in situ* via the hydrolysis of the solvent DMA, was confirmed by EA of the activated MOF 1a and from the ^1H NMR spectrum of 1a digested in $\text{DCl}/\text{D}_2\text{O}/\text{DMSO}-d_6$ solution (Fig. S2, ESI†).

The single crystal structure analysis showed that 1 is an anionic 3-D network composed of a dinuclear zinc cluster, $\text{Zn}_2(\text{COO})_5$, as an SBU of a 5-connected node and three different binding modes of two triscarboxylates, BTC^{3-} and BTB^{3-} , as three different 3-connected nodes (Fig. S3, ESI†).

The two $\text{Zn}(\text{II})$ ions of a tetrahedral coordination geometry in the $\text{Zn}_2(\text{COO})_5$ cluster are triply bridged with two different kinds of three triscarboxylates, two BTC^{3-} and a BTB^{3-} (Fig. 1a). The remaining coordination sites of the $\text{Zn}(\text{II})$ centers are completed by the monodentate carboxylates from two BTC^{3-} to form the SBU of a distorted trigonal bipyramidal 5-connected node. All three carboxylates of a BTB^{3-} on a crystallographic threefold axis are in a bridging binding mode and serve as a C_3 -symmetric 3-connected node (Fig. 1b). All three carboxylates of a BTC^{3-} on another crystallographic threefold axis are in a monodentate binding mode and serve as a C_3 -symmetric 3-connected node (Fig. 1c). Another BTC^{3-} with mixed binding modes of carboxylates, two carboxylates of bridging binding mode, and a carboxylate of monodentate binding mode, serves as the other 3-connected node in the network structure (Fig. 1d).

Topology analysis using TOPOS program²² reveals that the MOF is a 3-D network of an unprecedented 3,3,3,5-connected

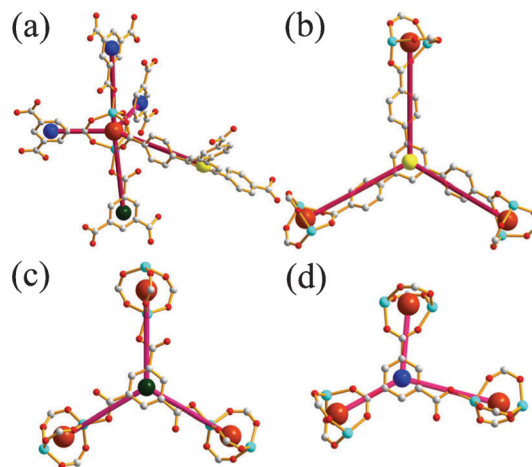


Fig. 1 A dinuclear zinc cluster as an SBU and three triscarboxylate ligands in three different environments in 1. (a) The dinuclear zinc cluster, $\text{Zn}_2(\text{COO})_5$, as a 5-connected node. (b) A BTB^{3-} as a 3-connected node. (c) A BTC^{3-} as a 3-connected node with all three carboxylates in monodentate binding mode. (d) Another BTC^{3-} as a 3-connected node with all three carboxylates in bidentate-binding mode.

net topology with [4576] transitivity and $\{4.6^3.8^6\}_3\{6^3\}\{8^3\}\{4.6^3.8^6\}_3$ point symbol. The only other MOF yet reported with the mixed rigid triscarboxylates BTC^{3-} and BTB^{3-} as ligands is the In-MOF, CPM-12, of the same 3,3,3,5-connected net topology, but with different [4576] transitivity and $\{4^2.6\}_3\{8^3\}_2\{4^2.6.8^4.10^3\}_3$ point symbol. In CPM-12, a dimeric $\text{In}_2(\text{OH})$ SBU serves as a 5-connected node and a BTC^{3-} , a pair of BTC^{3-} , and a pair of BTB^{3-} serve as three different kinds of 3-connected nodes.²³ Although the charge balance of the crystal structure strongly suggests that the framework of the MOF, $[(\text{Zn}_2)_3(\text{BTC})_4(\text{BTB})]^{3-}$, is an anionic network, it was not possible to identify any countercation in the crystal structure because the countercation was probably completely disordered in the solvent-filled pores. However, the EA result of 1a and the ^1H NMR data of the digested 1a under acidic conditions confirm the presence of dimethylammonium ion as a countercation in the network.

The MOF is a 3-D network with a complicated 3-D solvent pore structure. Careful examination of the 3-D solvent pores with the tile information from the topology analysis shows that the 3-D pores are composed of three different types of cage-like pores, A-cage, B-cage, and C-cage, and that these cage-like pores are interconnected to each other *via* a multiway channel to form the 3-D solvent pore structure.

The A-cage belonging to a local D_3 point group has an approximate spherical cavity of $\sim 8 \text{ \AA}$ in diameter and has six identical oval-shaped portals of dimensions $\sim 5 \times 10 \text{ \AA}^2$ (Fig. 2).

The B-cage belonging to a local S_6 point group has a disc-shaped cavity of $\sim 4 \text{ \AA}$ in height and $\sim 10 \text{ \AA}$ in diameter, and has six identical oval-shaped portals of dimensions $3.7 \times 4.3 \text{ \AA}^2$ (Fig. 3).

C-cage belongs to a D_3 point group as A-cage, but has a trigonal prismatic cavity of $\sim 10 \text{ \AA}$ in height and $\sim 16 \text{ \AA}$ in diameter and has six identical portals of dimensions $\sim 7 \times 9 \text{ \AA}^2$ (Fig. 4).

† An attempt to prepare the MOF using similar reaction conditions, but with reactants in the stoichiometric 6:4:1 ratio, only afforded an amorphous product.

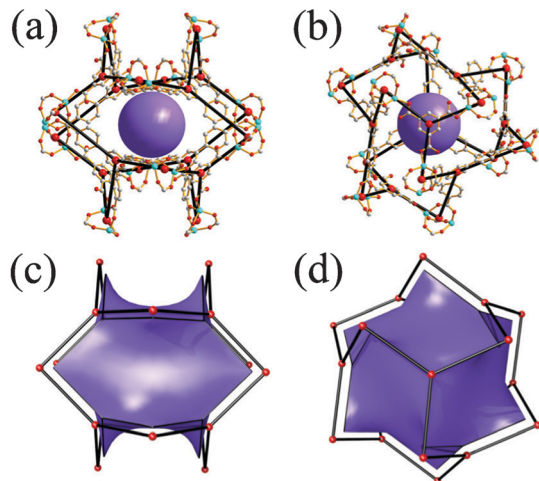


Fig. 2 Diagrams of A-cage on a crystallographic $32 (D_3)$ symmetry site. Ball-and-stick diagrams of the A-cage with nodes (medium-sized red balls) and edges (black stick) in (a) side and (b) top views, where the center of the A-cage is represented by a large purple dummy sphere. Tile diagrams of the A-cage with nodes (red balls), edges (black stick), and tiles (purple) in (c) side and (d) top views.

The cage-like pores in the network are interconnected *via* a ten-way channel (Fig. 5) to form a complicated 3-D porous structure. The channel structure is composed of two cyan tiles and four surrounding green tiles, and it has ten portals (Fig. 5b).

In the network, the pores of the A-cages are interconnected to each other *via* the channel through a necklike region $\sim 4 \text{ \AA}$ in diameter (Fig. 6a and 6b) to form a 3-D porous structure of a primitive cubic arrangement of the A-cages (Fig. 6c and 6d). The 3-D channel pores in the primitive cubic arrangement are twofold interpenetrated.

The pores of the four B-cages in a tetrahedral arrangement are also interconnected to each other *via* the same ten-way

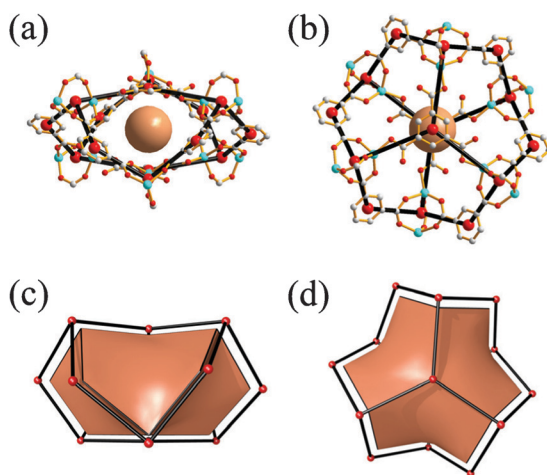


Fig. 3 Diagrams of B-cage on a crystallographic $\bar{3} (S_6)$ symmetry site. Ball-and-stick diagrams of the B-cage with nodes (medium-sized red balls) and edges (black stick) in (a) side and (b) top views, where the center of the B-cage is represented by a large brown dummy sphere. Tile diagrams of the B-cage with nodes (red balls), edges (black stick), and tiles (brown) in (c) side and (d) top views.

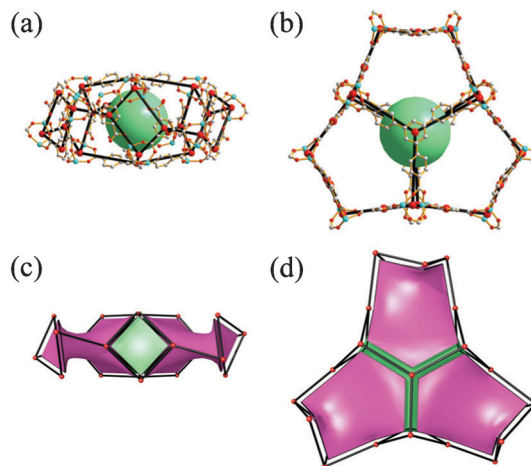


Fig. 4 Diagrams of C-cage on a crystallographic $32 (D_3)$ symmetry site. Ball-and-stick diagrams of the C-cage with nodes (medium-sized red balls) and edges (black stick) in (a) side and (b) top views, where the center of the C-cage is represented by a large green dummy sphere. Tile diagrams of the C-cage with nodes (red balls), edges (black stick), and tiles (green and pink) in (c) side and (d) top views, where the C-cage is composed of a green tile and three surrounding pink tiles.

channel (Fig. 7a and 7b), in four different directions, to form another 3-D channel porous structure (Fig. 7c and 7d).

The pores of the four C-cages in another tetrahedral arrangement are also interconnected to each other *via* the same ten-way channel (Fig. 8a and 8b), in four different directions, to form another 3-D channel structure (Fig. 8c and 8d).

Homogeneity and stability of the MOF

The combination of the optical microscopic photograph and the PXRD pattern of the bulk as-synthesized crystalline sample (Fig. S4 and S5, ESI[†]) provides supporting evidence that the sample is homogeneous and the single-crystal structure is representative of the bulk sample.

The PXRD pattern of the activated sample (1a) prepared under N_2 is similar to that of the as-synthesized sample (1), but the peaks are slightly broadened (Fig. S5, ESI[†]). When 1a

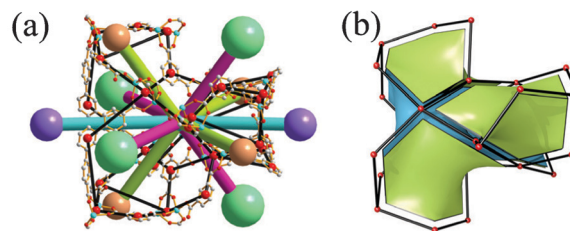


Fig. 5 Diagrams of a ten-way channel. (a) Ball-and-stick diagram of the channel with ten portals interconnecting ten cage-like pores (three differently colored large balls), where nodes are drawn as medium-sized red balls and edges as black sticks. (b) Tile diagram of the channel made of two different kinds of tiles (cyan and green). The second cyan tile and the fourth green tile are hidden by the green tile on the right side of the figure.

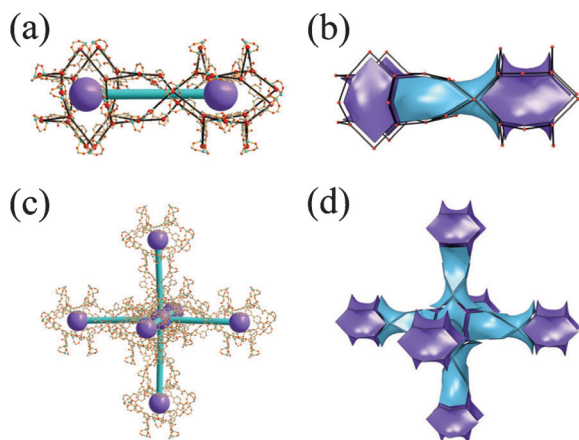


Fig. 6 Diagrams showing the connectivity between the pores of the A-cages. (a) Ball-and-stick diagram of two A-cages interconnected *via* a ten-way channel and (b) the corresponding tile diagram. (c) Ball-and-stick diagram of a central A-cage interconnected to the six surrounding A-cages in a primitive cubic-packing arrangement and (d) the corresponding tile diagram.

is res soaked in DMA, the original sharpness of the PXRD pattern is restored.

The TGA of **1a** exposed at ambient conditions for approximately 1 h shows multistep weight losses (Fig. S6, ESI[†]). The 1.8% weight loss up to 125 °C corresponds to the weight of three water molecules (1.9% calculated) readsorbed at ambient conditions, the next 1.0% weight loss up to 200 °C corresponds to the weight of 0.16 lattice DMA molecules (0.9% calculated) in the solvent pore, and then the decomposition of the framework commences at around 230 °C. The TGA results also support the presence of a small amount of lattice DMA in the solvent pore. Even though the MOF was soaked

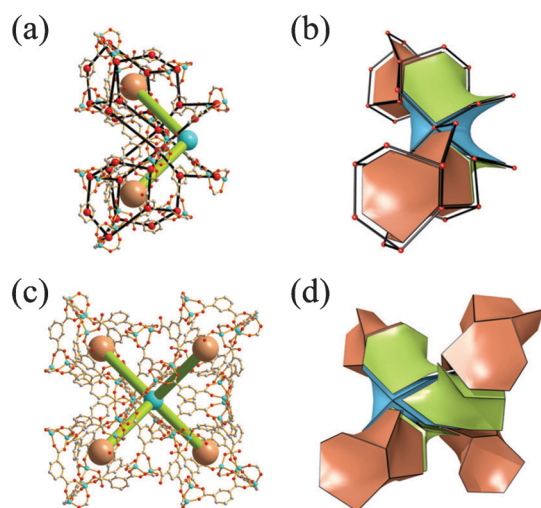


Fig. 7 Diagrams showing the connectivity between the pores of B-cages. (a) Ball-and-stick diagram of two B-cages interconnected *via* a ten-way channel and (b) the corresponding tile diagram. (c) Ball-and-stick diagram of four B-cages interconnected to each other *via* the ten-way channel in a tetrahedral arrangement and (d) the corresponding tile diagram.

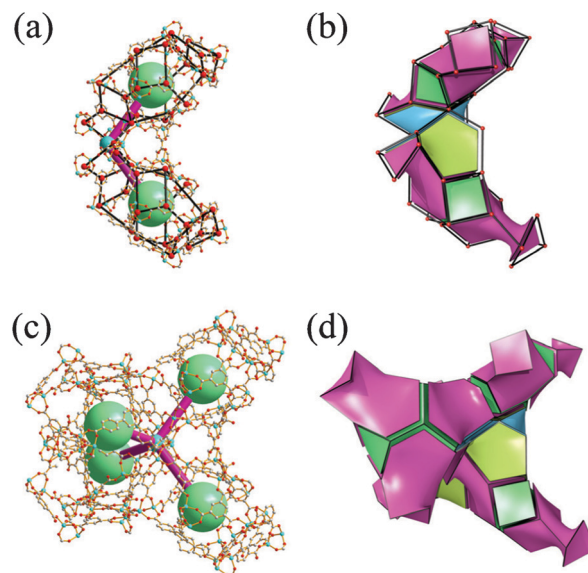


Fig. 8 Diagrams showing the connectivity between the pores of C-cages. (a) Ball-and-stick diagram of two C-cages interconnected *via* a ten-way channel and (b) the corresponding tile diagram. (c) Ball-and-stick diagram of four C-cages interconnected to each other *via* the ten-way channel in another tetrahedral arrangement and (d) the corresponding tile diagram. The three different kinds of cage-like pores are interconnected to each other *via* ten-way channels to form the complex 3-D channel porous structure.

in volatile acetone and the acetone was refreshed more than ten times during the 4 days of soaking, the lattice DMA molecules in the solvent pore were not completely replaced by acetone, probably because of the labyrinth of the pore in the narrow channel.

Gas sorption behaviour

The N₂ adsorption isotherm of **1a** is a typical type I isotherm of a microporous material (Fig. 9), which agrees with the solvent pore characteristics of the single-crystal structure of **1**.

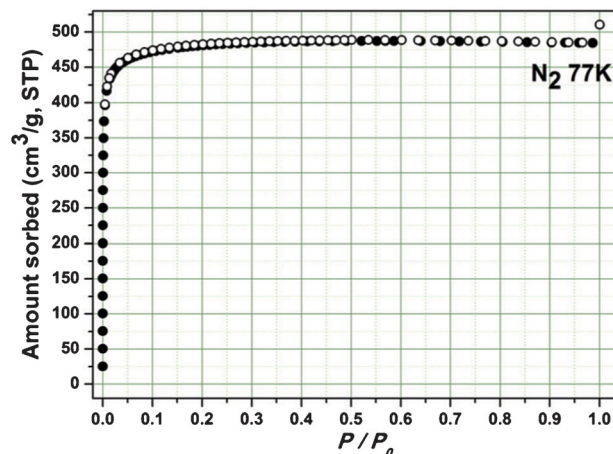


Fig. 9 N₂ sorption isotherms on **1a** at 77 K.

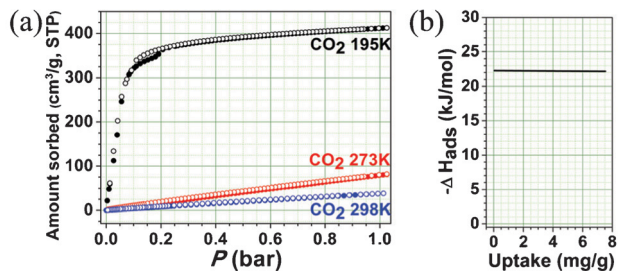


Fig. 10 (a) CO₂ sorption isotherms on **1** at 195, 273, and 298 K. (b) The adsorption enthalpy of CO₂.

The N₂ uptake amount is 485 cm³ g⁻¹ at $P/P_0 = 0.99$ and the BET- and Langmuir-specific surface areas are 1870 m² g⁻¹ and 2120 m² g⁻¹, respectively (Fig. S7 and S8, ESI†). The pore volume based on the N₂ uptake amount, 0.754 cm³ g⁻¹,[§] is slightly smaller than the estimated value based on the single-crystal structure, 0.813 cm³ g⁻¹.[¶] The median pore width of the framework calculated from the N₂ adsorption isotherm using the Saito–Foley cylindrical model is 11.8 Å.²⁴

The isotherms of CO₂ on **1a** at 195 K show stepwise adsorption at around 0.19 bar and hysteresis on desorption in the 0.1–0.2 bar range (Fig. 10a). The total CO₂ uptake amount at 1 bar is 413 cm³ g⁻¹ (81.1 mg g⁻¹). The origin of the hysteresis is not clear considering the rigidity and the microporosity of the framework. It is probably related the narrow channel structure of the pore. The adsorption enthalpy obtained from the CO₂ adsorption isotherms at 195, 273, and 298 K using a virial equation is ~22 kJ mol⁻¹ (ref. 25) and the value is in the expected range of the CO₂

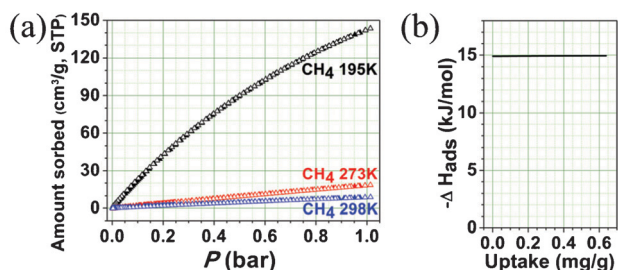


Fig. 11 (a) CH₄ sorption isotherms on **1** at 195, 273, and 298 K. (b) The adsorption enthalpy of CH₄.

[§] The pore volume of the MOF was calculated from the N₂ adsorption amount assuming that the density of N₂ in the pore at 77 K and 1 bar is the same as the density of liquid N₂, 0.813 cm³ g⁻¹.

[¶] In the calculation of the pore volume from the crystal structure, the volume of the dimethylammonium cation disordered in the solvent pore was estimated from the average atom volume derived by the analysis of the Cambridge Structural Database. D. Walter and M. Hofmann, *Acta Crystallogr., Sect. B: Struct. Sci.*, 2002, B58, 489–493.

|| We speculate that a certain region of the pore is only accessible when the CO₂ pressure is larger than ~0.19 bar *via* the narrow channel that is blocked by either the dimethylammonium cation in the pore or the DMF solvent remaining in the pore even after the activation of the sample.

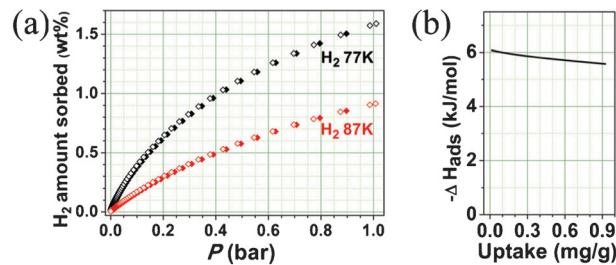


Fig. 12 (a) H₂ sorption isotherms on **1** at 77 and 87 K. (b) The adsorption enthalpy of H₂.

adsorption enthalpy of similar microporous MOFs with no open metal sites and no strongly interacting functional groups, such as an amino group.²⁶

The sorption behaviour of CH₄ on **1a** also agrees with the solvent pore characteristics of **1** from the single-crystal structure. The adsorption amounts of CH₄ on **1a** (144, 18, and 9 cm³ g⁻¹ at 195, 273, and 298 K, respectively) are much smaller than the corresponding adsorption amounts of CO₂ at the same temperatures (413, 81, and 38 cm³ g⁻¹ at 195, 273, and 298 K, respectively) (Fig. 11a). The adsorption enthalpy of CH₄ is ~15 kJ mol⁻¹. The selectivity of CO₂/CH₄ at 195, 273, and 298 K is 2.9, 4.5, and 4.2, respectively.

The adsorption amounts (1.6 and 0.9 wt% at 77 and 87 K, respectively) and the adsorption enthalpy (5–6 kJ mol⁻¹) of H₂ on **1a** are also the values in the expected range of the MOFs with similar specific surface area and microporosity (Fig. 12a).²⁷

Conclusions

While reaction of the Zn(II) ion with rigid H₂BTC and H₃BTB afforded 3,6-connected UMCM-1 using a Zn₄O(COO)₆ cluster as a 6-connected node, a similar reaction with rigid H₃BTC and H₃BTB resulted in a complicated 3-D network of an unprecedented 3,3,3,5-connected net topology using a structurally rare Zn₂(COO)₅ cluster as a 5-connected node. The highly porous 3-D network contains three different kinds of cage-like micropores interlinked to each other through a ten-way channel with narrow portals to form a complicated 3-D channel porous structure. The solvent molecules in the complicated 3-D channel pores could be removed by conventional vacuum drying with retention of the microporosity of the network, even though the solvent pore volume is larger than ~60% of the total unit cell volume. The MOF with no open metal sites and no strongly interacting functional organic residues in the pore surface shows the expected gas sorption behaviour, which corresponds to the BET-specific surface area and the average pore dimension of the network.

Acknowledgements

This work was supported by NRF-2010-0019408 and NRF-2012R1A2A2A01003077 through the National Research

Foundation of Korea. The authors acknowledge PAL for beam line use (2012-3rd-2D-012).

Notes and references

- M. O'Keeffe and O. M. Yaghi, *Chem. Rev.*, 2012, **112**, 675–702.
- (a) B. Chen, M. Eddaoudi, T. M. Reineke, J. W. Kampf, M. O'Keeffe and O. M. Yaghi, *J. Am. Chem. Soc.*, 2000, **122**, 11559–11560; (b) S. A. Bourne, J. Lu, A. Mondal, B. Moulton and M. J. Zaworotko, *Angew. Chem., Int. Ed.*, 2001, **40**, 2111–2113; (c) M. Eddaoudi, J. Kim, M. O'Keeffe and O. M. Yaghi, *J. Am. Chem. Soc.*, 2002, **124**, 376–377; (d) X. S. Wang, S. Ma, P. M. Forster, D. Yuan, J. Eckert, J. J. Lopez, B. J. Murphy, J. B. Parise and H.-C. Zhou, *Angew. Chem., Int. Ed.*, 2008, **47**, 7263–7266; (e) F. Nouar, J. F. Eubank, T. Bousquet, L. Wojtas, M. J. Zaworotko and M. Eddaoudi, *J. Am. Chem. Soc.*, 2008, **130**, 1833–1835; (f) X. Liu, M. Park, S. Hong, M. Oh, J. W. Yoon, J. S. Chang and M. S. Lah, *Inorg. Chem.*, 2009, **48**, 11507–11509; (g) J.-R. Li, J. Timmons and H.-C. Zhou, *J. Am. Chem. Soc.*, 2009, **131**, 6368–6369; (h) H. N. Wang, X. Meng, G. S. Yang, X. L. Wang, K. Z. Shao, Z. M. Su and C. G. Wang, *Chem. Commun.*, 2011, **47**, 7128–7130; (i) K. Seki, *Chem. Commun.*, 2001, 1496–1497; (j) K. Seki and W. Mori, *J. Phys. Chem. B*, 2002, **106**, 1380–1385; (k) R. Kitaura, K. Seki, G. Akiyama and S. Kitagawa, *Angew. Chem., Int. Ed.*, 2003, **42**, 428–431; (l) X. Song, T. K. Kim, H. Kim, D. Kim, S. Jeong, H. R. Moon and M. S. Lah, *Chem. Mater.*, 2012, **24**, 3065–3073.
- S. S.-Y. Chui, S. M.-F. Lo, J. P. H. Charmant, A. G. Orpen and I. D. Williams, *Science*, 1999, **283**, 1148–1150.
- B. Chen, M. Eddaoudi, S. T. Hyde, M. O'Keeffe and O. M. Yaghi, *Science*, 2001, **291**, 1021–1023.
- (a) D. Sun, S. Ma, Y. Ke, D. J. Collins and H.-C. Zhou, *J. Am. Chem. Soc.*, 2006, **128**, 3896–3897; (b) S. Ma, D. Sun, M. Ambrogio, J. A. Fillinger, S. Parkin and H.-C. Zhou, *J. Am. Chem. Soc.*, 2007, **129**, 1858–1859; (c) X. S. Wang, S. Ma, D. Yuan, J. W. Yoon, Y. K. Hwang, J. S. Chang, X. Wang, M. R. Jorgensen, Y. S. Chen and H.-C. Zhou, *Inorg. Chem.*, 2009, **48**, 7519–7521; (d) X.-S. Wang, S. Ma, D. Sun, S. Parkin and H.-C. Zhou, *J. Am. Chem. Soc.*, 2006, **128**, 16474–16475.
- (a) P. Wu, J. Wang, C. He, X. Zhang, Y. Wang, T. Liu and C. Duan, *Adv. Funct. Mater.*, 2012, **22**, 1698–1703; (b) L. Rajput, D. Kim and M. S. Lah, *CrystEngComm*, 2013, **15**, 259–264.
- (a) S. Amirjalayer, M. Tafipolsky and R. Schmid, *J. Phys. Chem. C*, 2011, **115**, 15133–15139; (b) H. Furukawa, Y. B. Go, N. Ko, Y. K. Park, F. J. Uribe-Romo, J. Kim, M. O'Keeffe and O. M. Yaghi, *Inorg. Chem.*, 2011, **50**, 9147–9152.
- (a) H. Li, M. Eddaoudi, M. O'Keeffe and O. M. Yaghi, *Nature*, 1999, **402**, 276–279; (b) M. Eddaoudi, J. Kim, N. Rosi, D. Vodak, J. Wachter, M. O'Keeffe and O. M. Yaghi, *Science*, 2002, **295**, 469–472; (c) H. K. Chae, D. Y. Siberio-Pérez, K. Jaheon, Y. B. Go, M. Eddaoudi, A. J. Matzger, M. O'Keeffe and O. M. Yaghi, *Nature*, 2004, **427**, 523–527; (d) H. K. Chae, J. Kim, O. D. Friedrichs, M. O'Keeffe and O. M. Yaghi, *Angew. Chem., Int. Ed.*, 2003, **42**, 3907–3909; (e) L. Rajput, S. Hong, X. Liu, M. Oh, D. Kim and M. S. Lah, *CrystEngComm*, 2011, **13**, 6926–6929.
- (a) H. Li, C. E. Davis, T. L. Groy, D. G. Kelley and O. M. Yaghi, *J. Am. Chem. Soc.*, 1998, **120**, 2186–2187; (b) C. A. Williams, A. J. Blake, P. Hubberstey and M. Schroder, *Chem. Commun.*, 2005, 5435–5437; (c) J. Y. Lee, L. Pan, S. P. Kelly, J. Jagiello, T. J. Emge and J. Li, *Adv. Mater.*, 2005, **17**, 2703–2706; (d) S. J. Garibay, J. R. Stork, Z. Wang, S. M. Cohen and S. G. Telfer, *Chem. Commun.*, 2007, 4881–4883.
- (a) H. Li, M. Eddaoudi, T. L. Groy and O. M. Yaghi, *J. Am. Chem. Soc.*, 1998, **120**, 8571–8572; (b) M. E. Braun, C. D. Steffek, J. Kim, P. G. Rasmussen and O. M. Yaghi, *Chem. Commun.*, 2001, 2532–2533; (c) D. N. Dybtsev, H. Chun and K. Kim, *Angew. Chem., Int. Ed.*, 2004, **43**, 5033–5036; (d) H. Chun, D. N. Dybtsev, H. Kim and K. Kim, *Chem.-Eur. J.*, 2005, **11**, 3521–3529; (e) Y. Zou, M. Park, S. Hong and M. S. Lah, *Chem. Commun.*, 2008, 2340–2342; (f) S. Hong, M. Oh, M. Park, J. W. Yoon, J. S. Chang and M. S. Lah, *Chem. Commun.*, 2009, 5397–5399; (g) H. Chun, *J. Am. Chem. Soc.*, 2008, **130**, 800–801; (h) J. I. Feldblyum, M. Liu, D. W. Gidley and A. J. Matzger, *J. Am. Chem. Soc.*, 2011, **133**, 18257–18263; (i) X. Song, S. Jeong, D. Kim and M. S. Lah, *CrystEngComm*, 2012, **14**, 5753–5755.
- (a) O. M. Yaghi, C. E. Davis, G. Li and H. Li, *J. Am. Chem. Soc.*, 1997, **119**, 2861–2868; (b) M. Eddaoudi, H. Li and O. M. Yaghi, *J. Am. Chem. Soc.*, 2000, **122**, 1391–1397; (c) X.-R. Hao, X.-L. Wang, K.-Z. Shao, G.-S. Yang, Z.-M. Su and G. Yuan, *CrystEngComm*, 2012, **14**, 5596–5603; (d) M. Oh, L. Rajput, D. Kim, D. Moon and M. S. Lah, *Inorg. Chem.*, 2013, **52**, 3891–3899; (e) Y. P. He, Y. X. Tan, F. Wang and J. Zhang, *Inorg. Chem.*, 2012, **51**, 1995–1997.
- C. Wang and W. Lin, *J. Am. Chem. Soc.*, 2011, **133**, 4232–4235.
- (a) M. H. Mir, L. L. Koh, G. K. Tan and J. J. Vittal, *Angew. Chem., Int. Ed.*, 2010, **49**, 390–393; (b) X.-L. Wang, C. Qin, E.-B. Wang and Z.-M. Su, *Chem.-Eur. J.*, 2006, **12**, 2680–2691; (c) Y.-Q. Lan, S.-L. Li, J.-S. Qin, D.-Y. Du, X.-L. Wang, Z.-M. Su and Q. Fu, *Inorg. Chem.*, 2008, **47**, 10600–10610; (d) P. K. Thallapally, J. Tian, M. R. Kishan, C. A. Fernandez, S. J. Dalgarno, P. B. McGrail, J. E. Warren and J. L. Atwood, *J. Am. Chem. Soc.*, 2008, **130**, 16842–16843; (e) J. M. Roberts, B. M. Fini, A. A. Sarjeant, O. K. Farha, J. T. Hupp and K. A. Scheidt, *J. Am. Chem. Soc.*, 2012, **134**, 3334–3337; (f) H. X. Zhang, F. Wang, H. Yang, Y. X. Tan, J. Zhang and X. Bu, *J. Am. Chem. Soc.*, 2011, **133**, 11884–11887; (g) A. Lan, K. Li, H. Wu, D. H. Olson, T. J. Emge, W. Ki, M. Hong and J. Li, *Angew. Chem., Int. Ed.*, 2009, **48**, 2334–2338; (h) H. Sato, R. Matsuda, M. H. Mir and S. Kitagawa, *Chem. Commun.*, 2012, **48**, 7919–7921; (i) Z. H. Zhang, S. C. Chen, J. L. Mi, M. Y. He, Q. Chen and M. Du, *Chem. Commun.*, 2010, **46**, 8427–8429; (j) B. Chen, S. Ma, E. J. Hurtado, E. B. Lobkovsky and H.-C. Zhou, *Inorg. Chem.*, 2007, **46**, 8490–8492; (k) Q. Y. Liu, Y. L. Wang, Z. M. Shan, R. Cao, Y. L. Jiang, Z. J. Wang and E. L. Yang, *Inorg. Chem.*, 2010, **49**,

- 8191–8193; (l) H. Park, J. F. Britten, U. Mueller, J. Lee, J. Li and J. B. Parise, *Chem. Mater.*, 2007, **19**, 1302–1308; (m) B. Chen, C. Liang, J. Yang, D. S. Contreras, Y. L. Clancy, E. B. Lobkovsky, O. M. Yaghi and S. Dai, *Angew. Chem., Int. Ed.*, 2006, **45**, 1390–1393; (n) L. Hou, Y.-Y. Lin and X.-M. Chen, *Inorg. Chem.*, 2008, **47**, 1346–1351; (o) S. Zheng, T. Wu, J. Zhang, M. Chow, R. A. Nieto, P. Feng and X. Bu, *Angew. Chem., Int. Ed.*, 2010, **49**, 5362–5366; (p) H. J. Park, Y. E. Cheon and M. P. Suh, *Chem.–Eur. J.*, 2010, **16**, 11662–11669; (q) D. Han, F. L. Jiang, M. Y. Wu, L. Chen, Q. H. Chen and M. C. Hong, *Chem. Commun.*, 2011, **47**, 9861–9863; (r) S. Henke and R. A. Fischer, *J. Am. Chem. Soc.*, 2011, **133**, 2064–2067; (s) K. L. Mulfort and J. T. Hupp, *J. Am. Chem. Soc.*, 2007, **129**, 9604–9605.
- 14 (a) H. Deng, C. J. Doonan, H. Furukawa, R. B. Ferreira, J. Towne, C. B. Knobler, B. Wang and O. M. Yaghi, *Science*, 2010, **327**, 846–850; (b) K. Koh, J. D. Van Oosterhout, S. Roy, A. G. Wong-Foy and A. J. Matzger, *Chem. Sci.*, 2012, **3**, 2429–2432; (c) Q. Yao, J. Su, O. Cheung, Q. Liu, N. Hedin and X. Zou, *J. Mater. Chem.*, 2012, **22**, 10345–10351.
- 15 (a) K. Koh, A. G. Wong-Foy and A. J. Matzger, *Angew. Chem., Int. Ed.*, 2008, **47**, 677–680; (b) Z. Wang, K. K. Tanabe and S. M. Cohen, *Inorg. Chem.*, 2009, **48**, 296–306; (c) K. Koh, A. G. Wong-Foy and A. J. Matzger, *J. Am. Chem. Soc.*, 2009, **131**, 4184–4185; (d) K. Koh, A. G. Wong-Foy and A. J. Matzger, *J. Am. Chem. Soc.*, 2010, **132**, 15005–15010; (e) H. Furukawa, N. Ko, Y. B. Go, N. Aratani, S. B. Choi, E. Choi, A. O. Yazaydin, R. Q. Snurr, M. O’Keeffe, J. Kim and O. M. Yaghi, *Science*, 2010, **329**, 424–428; (f) W. Chen, J.-Y. Wang, C. Chen, Q. Yue, H.-M. Yuan, J.-S. Chen and S.-N. Wang, *Inorg. Chem.*, 2003, **42**, 944–946; (g) L. Hou, J.-P. Zhang and X.-M. Chen, *Cryst. Growth Des.*, 2009, **9**, 2415–2419.
- 16 R. Grunker, V. Bon, A. Heerwig, N. Klein, P. Muller, U. Stoeck, I. A. Baburin, U. Mueller, I. Senkovska and S. Kaskel, *Chem.–Eur. J.*, 2012, **18**, 13299–13303.
- 17 *Materials Studio, version 4.3*, Accelrys, San Diego, CA, 2008.
- 18 A. J. Arvai and C. Nielsen, *ADSC Quantum-210 ADX Program*, Poway, CA, USA, 1983.
- 19 W. Minor, M. Cymborowski, Z. Otwinowski and M. Chruszcz, *Acta Crystallogr., Sect. D: Biol. Crystallogr.*, 2006, **62**, 859–866.
- 20 G. M. Sheldrick, *Acta Crystallogr., Sect. A*, 2008, **64**, 112.
- 21 A. L. Spek, *Acta Crystallogr., Sect. D: Biol. Crystallogr.*, 2009, **65**, 148–155.
- 22 V. A. Blatov, *IUCr CompComm Newsletter*, 2006, **7**, 4–38, TOPOS is available at <http://www.topos.ssu.samara.ru/>.
- 23 S.-T. Zheng, J. J. Bu, T. Wu, C. Chou, P. Feng and X. Bu, *Angew. Chem., Int. Ed.*, 2011, **50**, 8858–8862.
- 24 A. Saito and H. C. Foley, *AIChE J.*, 1991, **37**, 429–436.
- 25 (a) L. Czepirski and J. Jagiello, *Chem. Eng. Sci.*, 1989, **44**, 797–801; (b) J. Jagiello, T. J. Bandosz, K. Putyera and J. A. Schwarz, *J. Chem. Eng. Data*, 1995, **40**, 1288–1292; (c) A. Ansón, J. Jagiello, J. B. Parra, M. L. Sanjuán, A. M. Benito, W. K. Maser and M. T. Martínez, *J. Phys. Chem. B*, 2004, **108**, 15820–15826; (d) J. L. C. Rowsell and O. M. Yaghi, *J. Am. Chem. Soc.*, 2006, **128**, 1304–1315.
- 26 K. Sumida, D. L. Rogow, J. A. Mason, T. M. McDonald, E. D. Bloch, Z. R. Herm, T. H. Bae and J. R. Long, *Chem. Rev.*, 2012, **112**, 724–781.
- 27 M. P. Suh, H. J. Park, T. K. Prasad and D. W. Lim, *Chem. Rev.*, 2012, **112**, 782–835.